mp 104–105 °C), was used without further purification. ***trans*-1-(3-Methyl-2-naphthyl)-2-(2-naphthyl)ethene.** A sample of 2-(bromomethyl)-3-methylnaphthalene was converted to the corresponding phosphonium salt by treatment with triphenylphosphine in refluxing xylene. This salt was subjected to a Wittig reaction with 2-naphthaldehyde, by using a previously described phase-transfer method employing 50% aqueous sodium hydroxide and dichloromethane.[24] The crude solid product was digested with a 70/30 mixture of ethanol and water to remove the soluble triphenylphosphine oxide. The residual insoluble material was shown by GC/MS analysis to consist of a mixture of the cis and trans isomers of the desired alkene. This material was isomerized to the trans isomer by dissolving it in toluene containing a trace amount of iodine and irradiating the resulting solution with visible light. After the isomerization was shown to be complete by GC analysis, the solution was washed in a separatory funnel with aqueous 5% sodium thiosulfate solution, and the organic layer was separated, dried over anhydrous sodium sulfate, filtered, and rotary evaporated. The solid residue recrystallized twice from toluene to give *trans*-1-(3-methyl-2-naphthyl)-2-(2-naphthyl)ethene, mp 162.1–162.4 °C: ^{1}H NMR (200.1 MHz, $CDCl_3$) δ 8.103, 7.910, and 7.648 (br s, 1 H each, H-1, H-1′, H-4), 7.883–7.626 (complex m, 6 H), 7.506–7.384 (complex m, 4 H), 7.563 and 7.318 (AB q, 2 H, H-α and H-α', J = 16.1 Hz), 2.625 (s, 3 H, methyl). Anal. Calcd for $C_{23}H_{18}$: C, 93.84; H, 6.16. Found: C, 93.73; H, 6.20. ***trans*-1,2-Di(3-methyl-2-naphthyl)ethene.** A sample of 3.10 g (35 mmol) of 2-nitropropane dissolved in 5 mL of dry methanol was mixed with a solution prepared from the reaction of 0.83 g (36 mmol) of sodium with 30 mL of dry methanol. This material was stirred magnetically at room temperature while a solution of 6.56 g (28 mmol) of 2-(bromomethyl)-3-methylnaphthalene in 300 mL of dry methanol was added dropwise over 45 min. After the reaction mixture had been stirred for an additional 20 h, it was diluted with 250 mL of dichloromethane and washed in a separatory funnel with 2 100-mL portions of aqueous 10% sodium hydroxide solution and 1 200-mL portion of water. The organic layer was separated, dried over anhydrous magnesium sulfate, filtered, and rotary evaporated. The solid residue was recrystallized from 100 mL of hexane to give 3.24 g (68%) of off-white 3-methyl-2-naphthaldehyde, mp 118.0–119.2 °C (lit.[25] mp 124–125 °C). With the phase transfer method and the workup procedure described in the preceding paragraph, this aldehyde was subjected to a Wittig reaction with the phosphonium salt derived from the reaction of triphenylphosphine with 2-(bromomethyl)-3-methylnaphthalene. The crude product was recrystallized twice from toluene and then sublimed at 200 °C (0.005 Torr) to give *trans*-1,2-di(3-methyl-2-naphthyl)ethene as a faintly yellow solid with mp 218–219 °C: ^{1}H NMR (200.1 MHz, $CDCl_3$) δ 8.081 (s, 1 H, H-1), 7.859 (X part of ABX, 1 H, H-5 or H-8, $J_o + J_m$ = 9.5 Hz), 7.757 (X part of ABX, 1 H, H-8 or H-5, $J_o + J_m$ = 9.5 Hz), 7.659 (s, 1 H, H-4), 7.454 (s, 1 H, H-α), 7.431 (two coincident AB parts of ABX patterns, 2 H, H-6 and H-7, $J_o + J_m$ = 9.5 Hz), 2.626 (s, 3 H, methyl); MS, m/z 308 (M^+), 293, 278. Anal. Calcd for $C_{24}H_{20}$: C, 93.46; H, 6.54. Found: C, 93.24; H, 6.57.

General Procedures. Melting points were measured with a Thomas-Hoover oil-bath apparatus and are uncorrected. Elemental analyses were performed by M-H-W Laboratories, Phoenix, AZ. ^{1}H NMR spectra were determined at 17 °C in deuteriochloroform solution with tetramethylsilane as an internal standard using an IBM WP-200 SY spectrometer operating at 200.1 MHz. GC/MS analyses were carried out with a Hewlett-Packard 5890 gas chromatograph interfaced with a Hewlett-Packard 5970 mass selective detector. Sublimations at reduced pressure were accomplished as described elsewhere.[26] UV absorption measurements were carried out with a Perkin-Elmer Lambda 5 spectrophotometer. Luminescence measurements were made with a Hitachi/Perkin-Elmer fluorescence spectrometer as previously described.[16] PCA-SM calculations were also carried out as previously described.[16] Spectral input matrices, described in the Results section, consisted of uncorrected fluorescence spectra. Pure component fluorescence spectra were corrected for instrumental response, and fractional contributions were based on corrected spectra. Correction factors for fluorescence intensity values were empirically obtained at 0.5-nm intervals by the method described by Parker[27] employing a General Electric (no. 7429/36) tungsten lamp operated at 35 amperes. The spectral output of this lamp at various wavelengths had previously been determined relative to a National Bureau of Standards standardized tungsten lamp manufactured by The Eppley Laboratory Inc. (EPT-1109). Light from the tungsten lamp was reflected off a block of magnesium carbonate through a lens into the emission monochromator of the fluorescence spectrometer.

Acknowledgment. Work at Florida State University was supported by NSF Grant CHE-8713093.

Registry No. *trans*-DNE, 2753-11-9.

Supplementary Material Available: Graphs of eigenvectors, pure component spectra, and coefficient triangle for the DNE/O_2, 367-nm matrix (3 pages). Ordering information is given on any current masthead page.

(24) Warner, J. C.; Anastas, P. T.; Anselme, J. *J. Chem. Educ.* **1985**, *62*, 346.
(25) Shields, J. E.; Bornstein, J. *Chemistry and Industry* **1967**, 1404–1405.
(26) Mallory, F. B. *J. Chem. Educ.* **1962**, *39*, 261.
(27) Parker, C. A. *Photoluminescence of Solutions*; Elsevier: Amsterdam, 1968; pp 252–258.

Many-Body Potential for Molecular Interactions

Allison E. Howard, U. Chandra Singh,† Martin Billeter,‡ and Peter A. Kollman*

Contribution from the Department of Pharmaceutical Chemistry, University of California—San Francisco, San Francisco, California 94143. *Received June 11, 1987*

Abstract: We have included both atomic polarizability and nonadditive exchange repulsion terms to a molecular mechanical force field and then utilized this force field to calculate complexation enthalpies for a series of crown ethers and ions. Using this model for both uncomplexed and complexed crown ethers, we have been able to calculate relative conformation energies and cation complexation enthalpies in which the relative and absolute agreement to experimental values are satisfactory. These results provide further evidence of the merit in including many-body terms in molecular mechanical calculations for which highly polarizable atoms or ionic interactions are treated. It is anticipated this implementation may be especially significant for macromolecular systems of biological interest.

Crown ethers have fascinated scientists of different disciplines for a multitude of reasons since their discovery by Pederson.[1] They are of interest to some scientists because they may be thought of as model systems for the study of binding interactions as found in molecule/drug or enzyme/substrate complexes.[2] This was the rationale that first motivated Wipff, Weiner, and Kollman[3] to study the conformational flexibility and the cation and binding specificity in the interaction of 18-crown-6 with alkali-metal cations

† Current address: Laboratory of Molecular Biology, Scripps Clinic and Research Foundation, La Jolla, CA 92037.
‡ Current address: Institut für Molekularbiologie und Biophysik, ETH-Hönggerberg, CH-8093 Zürich, Switzerland.

(1) Pederson, C. J. *J. Am. Chem. Soc.* **1967**, *89*, 7017.
(2) Kellogg, R. M. In *Host Guest Complex Chemistry/Macrocycles*; Vögtle, F., Weber, E., Eds.; Springer-Verlag: New York, 1985.
(3) Wipff, G.; Weiner, P.; Kollman, P. *J. Am. Chem. Soc.* **1982**, *104*, 3249.

0002-7863/88/1510-6984$01.50/0

using the calculational technique of molecular mechanics.

Although Wipff et al.[3] were able to demonstrate that molecular mechanics could be used to qualitatively reproduce experimental data on ether/cation complexes, they found it necessary to use different charge models for the uncomplexed and the complexed molecules during the calculations. This was necessary because their force field electrostatic term included only pairwise point charge–point charge [monopole] interactions and thus could not accommodate the altered charge distribution that developed during complexation. The importance of including nonadditive terms in molecular simulations of other systems has been stressed previously.[4,5] Lybrand and Kollman[6] have suggested that the addition of a nonadditive term to the pairwise electrostatic interaction term would allow one to reproduce experimental crown–cation complexation enthalpies while using the same charge model for the uncomplexed and complexed species.

We have pursued that suggestion in this paper by including both atomic polarizability and a nonadditive exchange repulsion component in our molecular mechanical force field. This force field was then used to calculate the complexation enthalpies of the ethers I–IV with the cations V–VII. We felt that examination of the

H_3COCH_3 (I) $(CH_2CH_2O)_4$ (II) $(CH_2CH_2O)_5$ (III) $(CH_2CH_2O)_6$ (IV)

H_3O^+ (V) NH_4^+ (VI) $(CH_3)_3NH^+$ (VII)

energies of complexation involving compounds I–VII was most timely since recent experimental gas-phase complexation energies have been reported for several of these and similar complexes. Complexation enthalpies have recently been obtained[7] for acyclic ether, polyethers, and cyclic crown ethers interacting with oxonium, methoxonium, alkylammonium, and pyridinium cations by mass spectrometric measurements.

Methods

The molecular mechanics program AMBER[8] was used to evaluate the energies and structures of acyclic and cyclic ethers I–IV and cations V–VII. The force field used in this study is given in eq I. We used an

$$E_{total} = \sum_{bonds} \frac{K_r}{2}(r - r_{eq})^2 + \sum_{angles} \frac{K_\theta}{2}(\theta - \theta_{eq})^2 + \sum_{dihedrals} \sum_n \frac{V_n}{2}[1 + \cos(n\phi - \gamma)] + \sum_{i<j} \left[\frac{A_{ij}}{R_{ij}^{12}} - \frac{B_{ij}}{R_{ij}^{6}} \right] + \sum_{i<j\ 1\text{-}4\ terms} \left[\tfrac{1}{2} \left[\frac{A_{ij}}{R_{ij}^{12}} - \frac{B_{ij}}{R_{ij}^{6}} \right] \right] + \sum_{H\text{-}bonds} \left[\frac{C_{ij}}{R_{ij}^{12}} - \frac{D_{ij}}{R_{ij}^{10}} \right] + \sum_{i<j} \left[\frac{q_i q_j}{\epsilon R_{ij}} \right] + \sum_{i<j\ 1\text{-}4\ terms} \left[\tfrac{1}{2} \left[\frac{q_i q_j}{\epsilon R_{ij}} \right] \right] \quad (I)$$

all-atom approach;[9] that is, each of the hydrogen atoms was explicitly included in the force field. The bond stretching, angle bending, torsional, and van der Waals [VDW] parameters for compounds I–IV have previously been described,[9,10] and these parameters were used without modification. The parameters for cations V–VII were derived from prototypical compounds[9] and are listed in Table I. A constant dielectric, $\epsilon = 1$, was used in all calculations in order to simulate a gas-phase environment. A scale factor of 0.5 was used for 1–4 VDW and 1–4 electrostatic interactions, as described in ref 9.

In AMBER, nonbonded interactions between hydrogens bonded to heteroatoms and electronegative atoms can be set to zero, which has precedent in the studies of Hagler et al.,[11] or described with a 10–12 potential. We examine both possibilities here, with the 10–12 parameters used [A = 4019 kcal Å^{12}/mol, B = 1409 kcal Å^{10}/mol] characteristic of a weak short-range attraction of 0.5 kcal/mol.

Electrostatic potential [ESP] charges[12] were obtained from single-point ab initio calculations[13] at the STO-3G or 6-31G* levels. Those charges, which were used for compounds I–IV, came from ab initio calculations of I in the conformation in which the out-of-plane methyl hydrogens are staggered with respect to the opposite carbon–oxygen bond.[14] The ESP charges for compound I were derived from a 6-31G* calculation with scaling of the final charges such that the calculated dipole moment was equivalent to the experimental value.[15] This led to a charge of −0.295 for oxygen, −0.018 for the carbons, 0.067 for the in-plane hydrogens, and 0.050 for the out-of-plane hydrogen atoms. The charges for the monomeric unit, $-H_2COCH_2-$, of compounds II–IV were

Table I. Force Field Parameters for Cations V–VII[a]

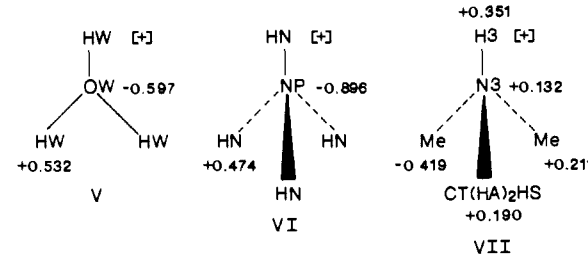

bond	K_r, kcal/mol·Å^2	r_{eq}, Å
HA–CT	340.0	1.088
HS–CT	340.0	1.109
CT–N3	337.0	1.451
N3–H3	376.0	1.000
HN–NP	376.0	1.012
OW–HW	550.0	0.973
angle	**K_θ, kcal/mol·rad^2**	**θ_{eq}, deg**
HA–CT–HS	35.0	108.11
HA–CT–N3	35.0	110.12
HA–CT–HA	35.0	108.58
CT–N3–H3	35.0	107.96
CT–N3–CT	40.0	110.94
HS–CT–N3	35.0	111.70
HN–NP–HN	70.0	109.47
HW–OW–HW	100.0	111.60
dihedral angle	**$V_n/2$, kcal/mol**	**γ, deg**	**n**
HA–CT–N3–H3	0.118	0.0	3
HS–CT–N3–H3	0.118	0.0	3
HS–CT–N3–H3	0.050	0.0	2
HA–CT–N3–CT	0.134	0.0	3
HS–CT–N3–CT	0.134	0.0	3
VDW	**R^*, Å**	**ϵ, kcal/mol**
HA	1.54	0.01
HS	1.54	0.01
N3	1.90	0.20
H3	1.00	0.02
NP	1.90	0.20
HN	1.00	0.02
OW	1.60	0.15
HW	1.00	0.02

[a] key: K_r, harmonic force constant for bond; r_{eq}, equilibrium bond length; K_θ, harmonic force constant for angle; θ_{eq}, equilibrium angle; $V_n/2$, half of the dihedral barrier height; γ, phase shift angle; n, periodicity of dihedral angle; R^*, VDW radius; ϵ, well depth of 6–12 potential.

(4) Warshel, A.; Levitt, M. *J. Mol. Biol.* **1976**, *103*, 227.
(5) Warshel, A. *J. Phys. Chem.* **1979**, *83*, 1640.
(6) Lybrand, T. P.; Kollman, P. A. *J. Chem. Phys.* **1985**, *83*, 2923.
(7) (a) Sharma, R. B.; Kebarle, P. *J. Am. Chem. Soc.* **1984**, *106*, 3913. (b) Meot-Ner, M. *J. Am. Chem. Soc.* **1983**, *105*, 4912. (c) Hiraoka, K.; Grimsrud, E. P.; Kebarle, P. *J. Am. Chem. Soc.* **1974**, *96*, 3359.
(8) (a) Singh, U. C.; Weiner, P. K.; Caldwell, J.; Kollman, P. A. AMBER 3.0, University of California—San Francisco, 1987. (b) Weiner, P. K.; Singh, U. C.; Kollman, P. A.; Caldwell, J.; Case, D. A. AMBER 2.0, University of California—San Francisco, 1985.
(9) (a) Weiner, S. J.; Kollman, P. A.; Nguyen, D. T.; Case, D. A. *J. Comp. Chem.* **1986**, *7*, 230. (b) Weiner, S. J.; Kollman, P. A.; Case, D. A.; Singh, U. C.; Ghio, C.; Alagona, G.; Profeta, S.; Weiner, P. *J. Am. Chem. Soc.* **1984**, *106*, 765.
(10) Billeter, M.; Howard, A. E.; Kollman, P. A.; Kuntz, I. D., submitted for publication in *J. Am. Chem. Soc.*
(11) Hagler, A.; Euler, E.; Lifson, S. *J. Am. Chem. Soc.* **1974**, *96*, 5319.
(12) Singh, U. C.; Kollman, P. A. *J. Comput. Chem.* **1984**, *5*, 129.
(13) Singh, U. C.; Kollman, P. A. *QCEP* **1982**, *2*, 17.
(14) Boggs, J. E.; Altman, M.; Cordell, F. R.; Dai, Y. *J. Mol. Struct.* **1983**, *94*, 373.
(15) The gas-phase dipole moment of dimethyl ether was determined to be 1.31 D in: Blukis, U.; Kasai, P. H.; Myers, R. J. *J. Chem. Phys.* **1963**, *38*, 2753.

Table II. Dihedral Angle Ranges of Crown Ethers II–IV

	CO-CC1	OC-CO1	CC-OC1	CO-CC2	OC-CO2	CC-OC2	CO-CC3	OC-CO3	CC-OC3	CO-CC4	OC-CO4	CC-OC4	CO-CC5	OC-CO5	CC-OC5	CO-CC6	OC-CO6	CC-OC6
IIa	a	g^-	g^+	a	g^+	a	a	g^-	g^+	a	g^+	a						
IIb	a	g^+	g^+	a	g^+	a	a	g^-	a	g^-	g^-	a						
IIc	a	g^+	g^+	a	g^+	g^+	a	g^+	g^+	g^-	g^-	a						
IId	a	g^+	g^+	a	g^+	g^+	a	g^+	g^+	a	g^+	g^+						
IIIa	a	g^-	a	a	g^+	a	a	g^-	a	a	g^+	a	a	g^-	g^-			
IIIb	a	g^-	g^+	a	g^+	a	a	g^+	a	a	g^-	g^-	a	g^-	a			
IIIc	a	g^-	g^-	a	g^-	a	a	g^-	g^-	a	g^-	g^-	a	g^-	a			
IIId	a	g^-	a	a	g^+	a	g^+	g^+	a	a	g^+	a	g^+	g^+	a			
IIIe	a	g^-	a	a	g^+	a	g^+	g^+	a	a	g^+	a	a	g^-	g^-			
IIIf	g^-	g^+	a	a	g^-	a	a	g^+	a	a	g^-	g^-	a	a	a			
IIIg	g^+	g^-	a	a	g^+	g^-	a	g^-	g^-	g^+	g^-	a	g^-	g^+	a			
IIIh	g^+	g^-	a	g^-	a	a	g^-	g^+	g^+	a	g^+	a	a	g^+	a			
IIIi	a	g^-	a	g^-	g^-	g^-	a	g^-	a	a	g^-	g^+	g^+	g^-	a			
IVa	a	a	a	a	g^+	a	a	g^-	a	a	g^+	a	a	g^-	a	a	g^+	g^-
IVb	g^+	g^+	g^+	a	g^+	a	g^+	g^+	a	a	g^-	a	a	g^+	a	a	g^-	g^-
IVc	a	g^-	a	a	g^+	a	a	g^+	a	a	g^-	a	a	g^+	a	a	g^+	a
IVd	a	g^-	a	a	g^+	g^-	g^-	a	a	a	g^-	a	a	g^+	g^-	g^-	a	a
IVe	a	g^-	a	a	g^+	a	a	g^-	a	a	g^+	a	a	g^-	a	a	g^+	a
IVf	a	g^+	a	a	g^-	g^+	a	a	a	a	g^-	a	a	g^+	g^-	a	a	a
IVg	a	g^+	a	a	g^+	a	a	g^-	g^-	a	g^-	a	a	g^-	a	a	g^+	g^+

obtained by using the wave function and nuclei of I and fitting the potential to partial charges on all the atoms except the two in-plane hydrogens, which are removed to make polymeric units from I. This seven-point ESP fit[12] was then scaled, as above, resulting in charges of −0.406 for the oxygen, +0.244 for the carbon, and −0.021 for the out-of-plane hydrogen atoms. The input structure to the ab initio calculations for V was from the calculations of Rodwell and Radom.[16] Both the STO-3G and 6-31G* levels of calculation provided the same charges on the hydrogen and oxygen atoms of +0.532 and −0.597, respectively. Compound VI[17,18] was found to have charges of −0.896 for the nitrogen atom and +0.474 for the hydrogen atoms at the 6-31G* level of theory. A 6-31G* ESP calculation of VII[17,19] produced charges of −0.419 for the methyl carbons, +0.190 for the methyl hydrogens, which were gauche to the N–H bond, and +0.211 for the methyl hydrogens trans to the N–H bond. The nitrogen charge was found to be +0.132, and the amine hydrogen charge was +0.351.

Several methods were used to obtain the starting input geometries to the AMBER minimization module. The starting geometries for the acyclic ether I and the cations V–VII were the same as those used during the calculations of the ESP charges. Compounds II–IV were constructed from the geometry parameters of the force field. Different conformations for these compounds were then generated by minimizing structures from AMBER molecular dynamics runs. In addition, several unique and low-energy conformations for III were found with the Billeter et al.[20] ELLIPSOID program. The conformations that were generated and described by Wipff et al.[3] provided further starting structures for IV. The starting conformations for ether/cation complexes were computer graphically modeled from structures associated with the ether local minima.

All degrees of freedom of compounds I–IV and their complexes with V–VII were minimized with the double-precision conjugate gradient method of the molecular mechanical program AMBER. The calculations converged to a root-mean-square gradient of less than 0.001 kcal Å^{-1}. After convergence, a normal-mode analysis was done for each local minimum conformer to ensure that the structure did not correspond to a saddle point on the energy surface.

The polarization contribution to the molecular mechanical total energy was incorporated in the manner of Lybrand and Kollman[6] and Singh and Kollman.[21] The total energy of a structure was first minimized with the force field of eq I. The induced dipoles for the minimized static structure were then calculated by solving eq II–IV iteratively, starting with $\vec{\mu}_i = 0$. The values for the atomic polarizabilities, α_i, were taken from Kang[22] and Applequist et al.[23] [vide infra]. The polarization energy was calculated as shown in eq V. A three-body exchange repulsion contribution

$$\vec{\mu}_i = \alpha_i \vec{E}_i \tag{II}$$

$$\vec{E}_j = \sum_{i \neq j} \frac{q_i \vec{r}_{ij}}{r_{ij}^3} + \sum_{i \neq j} \frac{\vec{\mu}_i \vec{r}_{ij}}{r_{ij}^5} \vec{r}_{ij} \tag{III}$$

$$\vec{E}_j^0 = \sum_{i \neq j} \frac{q_i \vec{r}_{ij}}{r_{ij}^3} \tag{IV}$$

$$E_{pol} = -\tfrac{1}{2} \sum_j \alpha_j [\vec{E}_j^0 \cdot \vec{E}_j] \tag{V}$$

to the force field, shown in eq VI, was also modeled after Lybrand and Kollman.[6] The quantities A, α, and β are variable parameters, and the distances r_{xy} refer to the cation [1] and ether oxygen [2 and 3] centers.

$$E(\text{three-body}) = A[(e^{-\alpha r_{12}})(e^{-\alpha r_{13}})(e^{-\beta r_{23}})] \tag{VI}$$

Results

(a) Uncomplexed Ethers. A thorough, but not exhaustive, attempt was made to search for low-energy conformations of compounds II–IV. Each molecule was first generated by the geometrical parameters of the AMBER force field and computer graphics modeling. The resulting structures were minimized by molecular mechanics and then subjected to constant-temperature [450 K] molecular dynamics. After every 20 ps of dynamics, the coordinates were saved and later minimized. Additional conformations were generated for compound III through the use of the ELLIPSOID algorithm.[20] The conformations for IV of Wipff et al.[3] were used as starting structures for the molecular dynamics simulations of this molecule, and we found no new structures of lower energy after "quenching" the molecular dynamics runs.

We chose a limited number of the lowest energy conformations of compounds II–IV to investigate in this study. The dihedral angles associated with the heavy atoms of these conformations [IIa–d, IIIa–i, IVa–g] have been catalogued as gauche [±] or anti[24] and are listed in Table II. Table III contains the AMBER

(16) Rodwell, W. R.; Radom, L. *J. Am. Chem. Soc.* **1981**, *103*, 2865.

(17) Binkley, J. S.; Frisch, M. J.; DeFrees, D. J.; Rahgavachari, K.; Whiteside, R. A.; Schlegel, H. B.; Fluder, E. M.; Pople, J. A. GAUSSIAN 82; Department of Chemistry, Carnegie-Mellon University: Pittsburgh, PA, 1982.

(18) The input structure was generated from a 6-31G** basis set geometry optimization, and this structure is given below in the form of a G82 archive:[17] \\1, 1 \N \H, 1, R\H, 1, R, 2, 109.471221 \H, 1, R, 2, 109.471221, 3, 109.471221, 1 \H, 1, R, 2, 109.471221, 3, 109.471221, −1 \\R = 1.011784 \HF = −56.5455298 \RMSD = 0.864D-09\ RMSF = 0.260D-04 \PG = TD\\.

(19) The input structure was generated from a 4-31G basis set geometry optimization, and this structure is given below in the form of a G82 archive:[17] \\1,1 \N\H, 1, NHP \C, 1, NC, 2, TH \C, 1, NC, 2, TH, 3, CV, 0 \C, 1, NC, 2, TH, 3, −CV, 0 \H, 3, HC, 1, HCN, 2, 180., 0 \H, 4, HC, 1, HCN, 2, 180., 0 \H, 5, HC, 1, HCN, 2, 180., 0 \H, 3, HC1, 1, HCN1, 6, HCH, 0 \H, 3, HC1, 1, HCN1, 6, −HCH, 0 \H, 4, HC1, 1, HCN1, 7, HCH, 0 \H, 4, HC1, 1, HCN1, 7, −HCH, 0 \H, 5, HC1, 1, HCN1, 8, HCH, 0 \H, 5, HC1, 1, HCN1, 8, −HCH, 0 \\NHP = 1.00792 \NC = 1.508363 \TH = 107.439242 \CV = 119.999996 \HC = 1.077043 \HCN = 108.454947 \HC1 = 1.076916 \HCN1 = 109.021124 \HCH = 119.883157 \HF = −173.398919 \RMSD = 0.510D-09 \RMSF = 0.140D-04 \PG = CS\\.

(20) Billeter, M.; Havel, T. F.; Wüthrich, K. *J. Comput. Chem.* **1987**, *8*, 132.

(21) Singh, U. C.; Kollman, P. A. *J. Comput. Chem.* **1986**, *7*, 718.

(22) Kang, Y. K. Ph.D. Dissertation, Korea Advanced Institute of Science and Technology, 1983.

(23) Applequist, J.; Carl, J. R.; Fung, K.-K. *J. Am. Chem. Soc.* **1972**, *94*, 2952.

(24) Dihedral angle definitions: gauche$^+$, 0° to +120°; anti, ±120° to 180°; gauche$^-$, 0° to −120°.

Table III. Molecular Mechanical Energies [kcal/mol] of Uncomplexed Ether Conformers I–IV[a]

I	II	III	IV
Total Energy of Selected Structures under Conditions A			
2.955[Ia]	20.802[IIa]	18.786[IIIa]	19.409[IVa]
2.955	*19.408*	*17.465*	*17.730*
	17.954[IIb]	20.599[IIIb]	24.379[IVb]
	16.617	*19.024*	*22.342*
	19.826[IIc]	21.955[IIIc]	20.948[IVc]
	18.429	*20.278*	*19.521*
	18.338[IId]	19.707[IIId]	18.825[IVd]
	17.109	*18.113*	*16.491*
		21.322[IIIe]	18.096[IVe]
		19.799	*16.728*
		18.043[IIIf]	**17.963**[IVf]
		16.359	***15.622***
		17.685[IIIg]	19.244[IVg]
		15.431	*17.638*
		18.564[IIIh]	
		16.576	
		18.614[IIIi]	
		16.556	
Total Energy of Selected Structures under Conditions B			
2.955[Ia]	20.802[IIa]	18.786[IIIa]	19.409[IVa]
2.955	*19.773*	*17.809*	*18.284*
	17.954[IIb]	20.599[IIIb]	24.379[IVb]
	16.977	*19.461*	*22.899*
	19.826[IIc]	21.955[IIIc]	20.948[IVc]
	18.842	*20.731*	*19.912*
	18.338[IId]	19.707[IIId]	18.825[IVd]
	17.485	*18.533*	*17.306*
		21.322[IIIe]	18.096[IVe]
		20.181	*17.108*
		18.043[IIIf]	**17.963**[IVf]
		16.900	***16.499***
		17.685[IIIg]	19.244[IVg]
		16.232	*18.096*
		18.564[IIIh]	
		17.316	
		18.614[IIIi]	
		17.123	

[a] The most stable conformer for each compound is shown in bold text. The AMBER total molecular mechanical energy excluding polarizability is shown in plain text while the total energy including the polarization contribution is shown in italics. The superscripts identify the compound and conformer. Atomic polarizabilities are given. A:[21] O, 0.664; C, 1.064; H, 0.386. B:[22] O, 0.465; C, 0.878; H, 0.135.

molecular mechanical total energies for each of these conformations.

The four lowest energy conformations that we found for compound II are of C_4 [IId], C_2 [IIa], C_i [IIb], and C_1 [IIc] symmetries. In contrast to Bovill et al.,[25] we find the C_i conformation—the conformation which is found in the crystal structure[26]—to be of lowest energy [Figure 1A]. Bovill et al.[25] calculated the conformation that is most stable in solution,[27] that of C_4 symmetry, to be their molecular mechanical "global" minimum; however, we find this conformation to be approximately 0.4 kcal/mol higher in energy. It is not unreasonable to expect that the C_i conformation should be more stable in the absence of solvation since, despite the unfavorable dihedral energy associated with two pseudocorners,[28] this conformation benefits from two stabilizing 1–5 CH···O interactions. The C_4 conformation suffers from the repulsion associated with having all oxygen dipoles oriented toward the center of the ring and the destabilization of four genuine corners.[28]

Unlike compound II, we find only structures of C_i and C_1 symmetries for III. The crystal structure for uncomplexed III

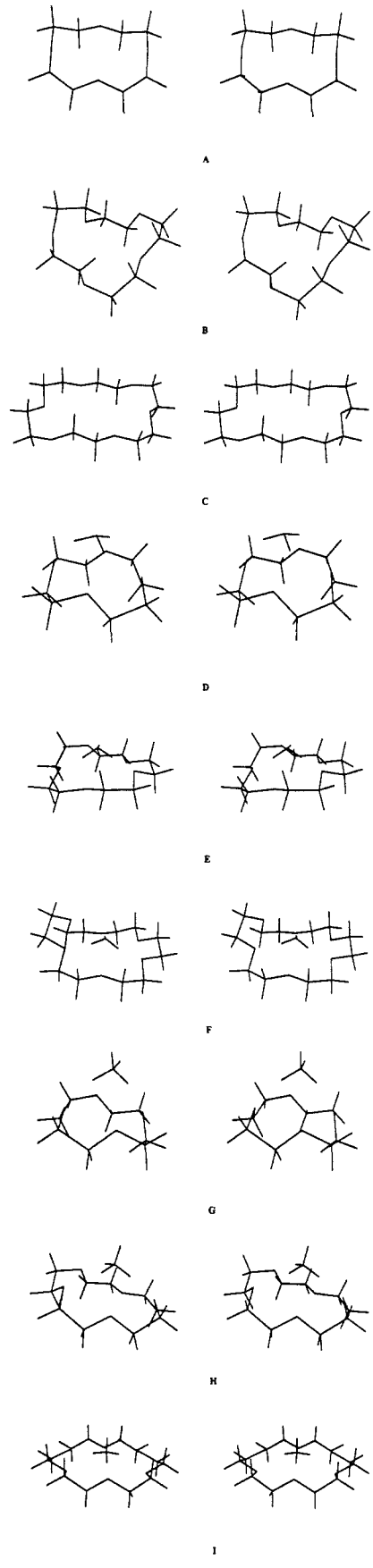

Figure 1. Stereoviews of the lowest energy molecular mechanical minimized conformers of 12-crown-4 [II], 15-crown-5 [III], and 18-crown-6 [IV] and their complexes with the oxonium [V], ammonium [VI], and trimethylammonium [VII] cations: A, IIb conformer; B, IIIg conformer; C, IVf conformer; D, IId/V complex; E, IIIa/V complex; F, IVb/V complex; G, IId/VI complex; H, IIIb/VI complex; I, IVe/VI complex; J, IId/VII complex; K, IIIe/VII complex; L, IVc/VII complex.

(25) Bovill, M. J.; Chadwick, D. J.; Sutherland, I. O. *J. Chem. Soc., Perkin Trans. 2* **1980**, 1529.
(26) Groth, P. *Acta Chem. Scand., Ser. A* **1978**, *A32*, 279.
(27) Anet, F. A. L.; Krane, J.; Dale, J.; Daasvatn, K.; Kristiansen, P. O. *Acta Chem. Scand.* **1973**, *27*, 3395.
(28) (a) Dale[24b] defines a pseudocorner as the unit g^+g^-a or g^-g^+a and a genuine corner as g^+g^+a or g^-g^-a. (b) Dale, J. *Isr. J. Chem.* **1980**, *20*, 3.

Table IV. Hydrogen Bonding Models for Ethers I–IV Complexed With V

	I	II	III	IV
Hydrogen Bond 10–12: A = 4019.0 kcal Å^{12} mol; B = 1409.0 kcal Å^{10}/mol				
energy[a] kcal/mol	−13.722[Ia]	−38.669[IId]	−50.756[IIId]	−55.573[IVe]
min HW–O dist,[b] Å	2.627	2.548	2.552	2.749
Hydrogen Bond 10–12: A = 0.0 kcal Å^{12} mol; B = 0.0 kcal Å^{10}/mol				
energy[a] kcal/mol	−15.266[Ia]	−37.490[IId]	−50.881[IIIa]	−54.040[IVb]
min HW–O dist,[b] Å	2.421	2.433	2.446	2.588

[a] AMBER molecular mechanical total energy of global minimum conformers. The polarization contribution is not included in the total energy. The superscripts refer to the conformer identities. [b] Minimum distance between the oxonium oxygen and an ether oxygen.

has not been determined although a structure has been proposed[28b] for the conformer that is believed to predominate in solution. Dale[28b] has suggested that this conformer is uniangular with two pseudocorners [g$^+$g$^+$a g$^+$g$^-$a ag$^+$a aaa g$^-$g$^+$a]. After extensive searching, we were not able to locate this conformation as a local minimum in our force field. In that region of conformational space, we did find a local minimum for a conformer similar to the one proposed by Dale.[28b] The energy of this conformer [g$^+$g$^+$a ag$^-$a ag$^+$g$^-$ aaa g$^-$g$^+$a] is approximately 0.7 kcal/mol less stable than the lowest energy conformer we found for III. Our lowest energy conformer [IIIg] is uniangular with three pseudocorners and, hence, three attractive 1–5 CH···O interactions [Figure 1B].

We calculate the lowest energy conformation for IV to be of C_i symmetry [IVf] [Figure 1C] and the D_{3d} conformation [IVe] to be of only slightly higher energy. The C_i conformation is stabilized by two transannular 1–5 CH···O interactions, which help to offset the poor dihedral energy contribution from the presence of two pseudocorners. The D_{3d} conformer contains an optimal sequence of dihedral angles but is destabilized by the repulsion of the oxygen atoms that are contained in the same plane. These calculational results are in agreement with the previous calculations of Wipff et al.[3] and experimental data.[28b,29] Bovill et al.[25] also calculate the C_i conformation to be the global minimum but find the D_{3d} conformation to be considerably less stable. With respect to the other conformers of IV, our results are quite similar to those of Wipff et al.[3] The major difference between the two sets of data is that we find the relative energy of the $C_{1'}$ conformer [IVa] to be 1.4 kcal/mol higher than the C_i conformer [IVf] while Wipff et al.[3] finds this difference to be only 0.7 kcal/mol.

The total energies of the ethers, with the inclusion of the polarization term, are also shown in Table III. Two sets of atomic polarizabilities have been investigated. The polarizabilities of Kang[22] have values of 0.664 for oxygen, 1.064 for carbon, and 0.386 for hydrogen while these values are 0.465, 0.878, and 0.135 with the Applequist et al.[23] model. The addition of the polarization term to the force field causes variable degrees of stabilization of the ether conformers, but the relative assignment of the global minima remains unchanged.

(b) H_3O^+/Ethers. The ether/oxonium complexes were constructed with computer graphics by placing the oxonium ion in an orientation near the approximate center of each crown ether conformer or, in the case of I, near the oxygen atom. We first evaluated the energies of these complexes using several hydrogen-bond models. The results of these calculations are shown in Table IV where only the global minimum for each complex has been listed.

We were able to select the most appropriate hydrogen-bonding parameters by comparing the experimental optimal O···H$^{\delta+}$···O distance[30] [2.41 Å] with the calculated Ia[O]···[$^{\delta+}$HO]V distance. A comparison of parts a and b of Table IV shows that a zero hydrogen-bond function leads to an O···O distance in Ia/V in better agreement with experiment, although the interaction energies are not very dependent on the hydrogen-bond function.

Table V shows the calculational and experimental values for the complexation energies of I–IV with V. Three models were used to determine the polarization energy contribution. In model A, no polarization term was added to the force field. In model B, the Kang[22] atomic polarizabilities were used for the ether atoms, while in model C, we used the Applequist et al.[23] values for the ether atomic polarizabilities. As a highly localized cation, V would be expected to have a very small polarizability, and we have therefore assumed its polarizability to be zero.

The three models consistently show the relative interaction energy of I/V, with respect to the II/V, III/V, and IV/V complexation energies, to be much smaller in magnitude compared to what is found experimentally.[7c] We suspected that the experimental[7c] value for the I/V complexation energy really corresponded to the interaction of I/H$^+$ + H_2O. In order to test this hypothesis, we determined the I/V complexation energy using a single-point 6-31G* basis set calculation after first optimizing the Ia[O]···[$^{\delta+}$HO]V distance at the 4-31G level. This calculation[13] found the complexation energy to be −35.631 kcal/mol, which is considerably smaller than the reported experimental value of −49.8 kcal/mol and in better agreement with the molecular mechanical results.

Both models B and C represent the absolute complexation energies better than does model A, but they place the relative complexation energy of III/V lower than IV/V, in disagreement with experiment.[7a] The model that uses the smaller atomic polarizabilities of Applequist et al.[23] appears to better mimic the complexation energies than that of Kang.[22]

The oxonium ion forms three hydrogen bonds with ether oxygens in the complexes II/V, III/V, and IV/V [parts D–F of Figure 1]. The crown ether of II/V was found to be of C_4 symmetry, unlike the uncomplexed ether but similar to the experimental X-ray structure of II/Na$^+$.[28b] The crown ethers of III/V and IV/V have similar geometries to each other; in each, all but one dihedral unit is of the form [a, g$^\pm$, a]. Sharma and Kebarle[7a] have proposed that V forms two strong and one partial hydrogen bond with III. We instead find one strong and two weaker hydrogen bonds in this complex [Figure 1E].

(c) NH_4^+/Ethers. The starting geometries for the complexes I–IV with VI were generated, as above, with computer graphics. Again, we chose hydrogen-bonding parameters of A = 0.0 kcal Å^{12}/mol and B = 0.0 kcal Å^{10}/mol. The complexation energies were evaluated by the three polarization models, and the results are given in Table V. All three models show the relative complexation energy to increase with the increasing size of the ether. However, the conformation of III, which represents the global minimum, is different when the polarization term is included than when polarization is not included in the force field. There are no gas-phase experimental results with which to compare our calculations for the complexation energies of the ethers with VI.

Unlike the crown ether/V complexes, the complexes of II and III with VI [parts G–I of Figure 1] contain only two hydrogen bonds between the ammonium hydrogens and ether oxygens. The macrocyclic ring in IV/VI is however large enough to accommodate the ion, and this complex contains three hydrogen bonds. The symmetry of the IV/VI complex is of the D_{3d} point group, and, in fact, this is the same structure as was found for the complex experimentally by X-ray crystallography.[31]

(d) $(CH_3)_3NH^+$/Ethers. After model building the complexes of I–IV with VII, we minimized the energies of the complexes and then used four polarization models to evaluate the complexation energies. As with the cations discussed above, model A contributed no polarization energy to the complexation energy and model C used Applequist et al.'s[23] atomic polarizabilities for the ether atoms, and the cation atomic polarizabilities were set equal to zero. Our two additional models placed polarizabilities of 0.878 on the amine carbons in model D, and in addition, model E also put an atomic polarizability of 0.525 on the amine nitrogen.

(29) Dunitz, J. D.; Seiler, P. *Acta Crystallogr., Sect. B: Struct. Crystallogr. Cryst. Chem.* **1974**, *B30*, 2739.
(30) Lundgren, J. O.; Olovson, I. *Acta Crystallogr.* **1967**, *23*, 966.
(31) Nagano, O.; Kobayashi, A.; Sasaki, Y. *Bull. Chem. Soc. Jpn.* **1978**, *51*, 790.

Table V. Computational and Experimental Complexation Enthalpies[a] of Ethers I–IV with Cations V–VII

	I	II	III	IV
		With V		
molecular mechanics[b]				
model A	$-18.22^{Ia/V}$	$-55.44^{IId/V}$	$-68.57^{IIIa/V}$	$-72.00^{IVb/V}$
model B	$-33.30^{Ia/V}$	$-88.43^{IId/V}$	$-106.29^{IIIa/V}$	$-101.33^{IVb/V}$
model C	$-28.29^{Ia/V}$	$-78.54^{IId/V}$	$-95.50^{IIIa/V}$	$-92.91^{IVb/V}$
experimental[c]			−76.9	−88.5
molecular mechanics with nonadditivity[d]		$-66.4^{IId/V}$	$-77.0^{IIIa/V}$	$-79.8^{IVb/V}$
		With VI		
molecular mechanics[b]				
model A	$-12.34^{Ia/VI}$	$-38.77^{IId/VI}$	$-46.72^{IIIb/VI}$	$-57.38^{IVe/VI}$
Model B	$-19.40^{Ia/VI}$	$-52.83^{IId/VI}$	$-63.04^{IIIb/VI}$	$-74.80^{IVe/VI}$
model C	$-16.92^{Ia/VI}$	$-47.92^{IId/VI}$	$-57.29^{IIIb/VI}$	$-68.74^{IVe/VI}$
experimental[c]				
		With VII		
molecular mechanics[b]				
model A	$-11.06^{Ia/VII}$	$-31.59^{IId/VII}$	$-32.64^{IIIe/VII}$	$-34.42^{IVc/VII}$
model C		$-35.60^{IId/VII}$	$-36.18^{IIIe/VII}$	$-38.58^{IVc/VII}$
model D		$-36.50^{IId/VII}$	$-37.14^{IIIe/VII}$	$-39.48^{IVc/VII}$
model E		$-36.80^{IId/VII}$	$-37.43^{IIIe/VII}$	$-39.75^{IVc/VII}$
experimental[c]	−19.5	−35.8	−34.9	−41 ± 4
molecular mechanics with nonadditivity[d]	$-34.2^{IId/VII}$	$-35.0^{IIIe/VII}$	$-37.5^{IVc/VII}$	

[a] In kilocalories per mole. [b] AMBER molecular mechanical enthalpies of complexation, which were calculated with the following atomic polarizabilities. Model A. Polarizability not included. Model B. Ethers: Oxygens, 0.664; carbons, 1.064; hydrogens, 0.386. Cations: no atomic polarizability. Model C. Ethers: oxygens, 0.465; carbons, 0.878; hydrogens, 0.135. Cations: no atomic polarizability. Model D. Ethers: oxygens, 0.465; carbons, 0.878; hydrogens, 0.135. Cations: carbons, 0.878; nitrogen, 0.000; hydrogens, 0.000. Model E. Ethers: oxygens, 0.465; carbons, 0.878; hydrogens, 0.135. Cations: carbons, 0.878; nitrogen, 0.525; hydrogens, 0.000. [c] References 7a and 7b; experimental value for I/V interaction is for H_2O···ether-H^+ not H_3O^+···ether complex. [d] Model C enthalpy energy + three-body exchange interaction term.

The molecular mechanical results for the complexation energies are shown in Table V.

The agreement between the experimental[7b] and calculated complexation energies for I–VI/VII is good, in contrast to what was found for the I–VI/V complexes. The addition of the polarization term in models C–E causes the absolute complexation energy to be within 10% of the experimental value for each of the complexes except Ia/VII.

As shown in parts J–L of Figure 1, the geometries of the crown ether/VII complexes are interesting and quite unlike those of the previously described complexes. Although the shortest O(ether)···HN(cation) distance is 2.2 Å in II/VII and thus only a weak hydrogen bond exists, considerable electrostatic interaction can occur between the ether oxygens and partially charged methyl hydrogens. This interaction is more strongly suggested in the larger III/VII and IV/VII complexes where the cation is canted, with respect to the crown ether ring, such that both $NH^{\delta+}$(cation)···O(ether) and $CH^{\delta+}$(cation)···O(ether) electrostatic interactions are maximized. This interaction has been previously proposed by Meot-Ner[7b] and is supported by both experimental[32] and theoretical[33] observations. We have also evaluated the complexation energy of a centrosymmetric IV/VII complex and found it to be approximately 5 kcal/mol less stable than the canted global minimum conformer IVc/VII, in further support of important $CH^{\delta+}$(cation)···O(ether) electrostatic interactions in these complexes. One could argue that one strong $NH^{\delta+}$(cation)···O(ether) interaction in the complex with "canted" VII is more favorable than six weak $NH^{\delta+}$(cation)···O(ether) interactions in the centrosymmetric D_{3d} complex, thus rationalizing the 5 kcal/mol preference. However, a molecular mechanical energy component analysis found that almost all of the 5 kcal/mol difference between the "canted" and centrosymmetric complexes comes from alkyl group···ether interactions.

(e) Nonadditive Force Field Component. When the polarization term is added to the force field during the calculations of I–VI/V, the relative energies for III/V and IV/V are no longer consistent with the experimental values. An examination and comparison of the structures suggested a possible cause for the change in relative energies. The total energy of the III/V complex benefits from a stabilizing and closer electrostatic interaction between two of the ether oxygens and one of the oxonium protons than is present in IV/V. We wondered if such an interaction would still contribute so strongly to the total energy of the complex if three-body exchange repulsion[6] was incorporated in the force field. For example, Lybrand and Kollman[6] have found in quantum mechanical calculations on cation–$(H_2O)_2$ complexes, where both waters are in the first coordination sphere of the cation, that there is an exchange repulsion three-body nonadditivity in the interaction. It is reasonable to expect that such a term might exist in cation···ether interactions, particularly when the distances between the cation and its oxygens and between the two oxygens are short. To test this hypothesis, we first evaluated the quantum mechanical and molecular mechanical energies for fragments of each complex.

For both the III/V and IV/V complexes, we chose the $(-H_2COCH_2-)_2$ fragment in which the oxygen(ether fragment)···H(cation)···oxygen(ether fragment) distances were the smallest. The original geometries of these fragments in the III/V and IV/V complexes were maintained, and two additional hydrogens were placed on each ether fragment, using standard geometries, to form 1,2-dimethoxyethane models. Similarly, both of these 1,2-dimethoxyethane models were further fragmented to form dimethyl ether models. The energies of these fragments, and appropriately placed oxonium ions, were then evaluated quantum mechanically[13] at the 4-31G level and also with the molecular mechanical model C of Table V, which included polarization. The results of these calculations are given in parts a and b of Table VI. The additional interaction energy nonadditivity was then calculated for each model, and these results are given in Table VII. Consistent with the shorter O···cation···O distances observed in III/V than IV/V, the repulsive nonadditivity calculated quantum mechanically for the model representing 15-crown-5 is larger than for the model representing 18-crown-6. These results support the idea that the excess stabilization of the III/V complex is associated with the calculation of only pairwise interactions and many-body polarization effects in the molecular mechanical model.

Of course, one needs to evaluate the three-body O···cation···O interactions for each possible triplet in III/V and IV/V to fully describe the total three-body nonadditivity. Given the uncertainties

(32) (a) Grimsrud, E. P.; Kebarle, P. *J. Am. Chem. Soc.* **1973**, *95*, 7939. (b) Meot-Ner, M. *J. Am. Chem. Soc.* **1978**, *100*, 4694. (c) Taylor, R.; Kennard, O. *J. Am. Chem. Soc.* **1982**, *104*, 5063.

(33) Hirao, K.; Sano, J.; Yamabe, S. *Chem. Phys. Lett.* **1982**, *87*, 181.

Table VI (a) Ab Initio Energies[a] of Selected Ether/V Fragments

fragments	molecule/complex	energy, Hartrees
	III/V	
1-3	$[(H_3COCH_2)_2/H_3O^+]$	-382.8052
1, 2	$[(H_3COCH_2)_2]$	-306.5144
1, 3	$[H_3COCH_3/H_3O^+]$	-230.0819
1	$[H_3COCH_3]$	-153.8364
2, 3	$[H_3COCH_3/H_3O^+]$	-230.0792
2	$[H_3COCH_3]$	-153.8351
3	$[H_3O^+]$	-76.1859
	IV/V	
1-3	$[(H_3COCH_2)_2/H_3O^+]$	-382.7982
1, 2	$[(H_3COCH_2)_2]$	-306.5146
1, 3	$[H_3COCH_3/H_3O^+]$	-230.0921
1	$[H_3COCH_3]$	-153.8355
2, 3	$[H_3COCH_3/H_3O^+]$	-230.0616
2	$[H_3COCH_3]$	-153.8366
3	$[H_3O^+]$	-76.1902

(b) Molecular Mechanical[a] Energies of Selected Ether/V Fragments

fragments	molecule/complex	energy, kcal/mol
	III/V	
1-3	$[(H_3COCH_2)_2/H_3O^+]$	-43.323
1, 2	$[(H_3COCH_2)_2]$	4.471
1, 3	$[H_3COCH_3/H_3O^+]$	-19.022
1	$[H_3COCH_3]$	4.229
2, 3	$[H_3COCH_3/H_3O^+]$	-20.861
2	$[H_3COCH_3]$	3.292
3	$[H_3O^+]$	0.996
	IV/V	
1-3	$[(H_3COCH_2)_2/H_3O^+]$	-35.095
1, 2	$[(H_3COCH_2)_2]$	4.261
1, 3	$[H_3COCH_3/H_3O^+]$	-20.425
1	$[H_3COCH_3]$	3.756
2, 3	$[H_3COCH_3/H_3O^+]$	-12.020
2	$[H_3COCH_3]$	3.206
3	$[H_3O^+]$	0.172

[a] Ab Initio[13] energies at 4-31G basis set level. [b] AMBER[8,9] molecular mechanical energies using model C of Table V. The listed energies for the complexes, molecules, and ions are enthalpies.

in the absolute values for the quantum and molecular mechanical models for the relative differences in nonadditivity of the III/V and IV/V complexes, we chose an alternate approach, catalyzed by the results of ref 6.

The results of the quantum and molecular mechanical calculations described above encouraged us to reevaluate the complexation energies of the crown ethers with the cations V and VII using eq IV, the form of which came from ref 6. Because of the limited data and only qualitative accuracy of the ab initio model we used, we kept the value of $\beta = 1.0$, similar to that used by Lybrand et al.[6] We then varied A and α to approximately reproduce the three-body nonadditivity differences found at the ab initio level for the single 15-crown-5 and 18-crown-6 O···cation···O geometries [Table VII]. We subsequently calculated the molecular mechanical energies for the full III/V interaction and empirically modified A to reproduce the absolute value of the interaction energy [see Table V]. The resulting final three-body parameters are $A = 440\,000$ kcal, $\alpha = 1.65$ Å^{-1}, and $\beta = 1.00$ Å^{-1}. The resulting relative complexation energies for III/V and IV/V are now in qualitative agreement with the experimental values. The preferential stabilization of the III/V complex compared to the IV/V complex is no longer seen, but the difference between the two complexation energies is still too small. To further test the reasonableness of our three-body exchange repulsion energy, we have included it in the interactions of VII with II-IV, where our previously described results were in good agreement with experiment. Encouragingly, the inclusion of this term there has little effect, because the distances between the cationic nitrogen and ether oxygen are significantly larger than found with H_3O^+ [V].

Discussion and Conclusions

We have been able to demonstrate that the addition of polarization energy to the total molecular mechanical energy allows one to utilize a consistent charge model for uncomplexed and complexed ethers. The inclusion of this term also allows better agreement between the computational and experimental values for the total complexation energies of ethers I-IV with cations V-VII. In addition, the inclusion of such a term does not greatly change the relative energies of the conformations of the crowns themselves, whose relative energies calculated in ref 3 and here are in rather good agreement with experiment. For example, our calculations find that the lowest energy structures for II, IV, and IV/VI are those observed crystallographically.

Table VII. Two- and Three-Body Complexation Contributions of III and IV Fragments with V

Ab Initio Model[a]	energy, kcal/mol
15-Crown-5	
sum of two-body interactions[b]	73.9
total three-body interactions[c]	65.8
nonadditivity[d]	8.1
18-Crown-6	
sum of two-body interactions[b]	63.5
total three-body interactions[c]	58.6
nonadditivity[d]	4.9
Molecular Mechanical Model[a]	**energy, kcal/mol**
15-Crown-5	
sum of two-body interactions[b]	49.4
actual triplet[c]	48.8
nonadditivity[d]	0.6
18-Crown-6	
sum of two-body interactions[b]	39.8
actual triplet[c]	39.5
nonadditivity[d]	0.3

[a] See text; this model does not include exchange repulsion. [b] {Fragments 1 & 3 [total energy(ether/oxonium ion) − (total energy(ether) + total energy(oxonium ion))] + fragments 2 & 3 [total energy(ether/oxonium ion) − (total energy(ether) + (total energy(oxonium ion))]}. [c] {Fragments 1-3 [total energy(ether/oxonium ion) − (total energy(ether) + total energy(oxonium ion))]. [d] Two-body energy − three-body energy.

The calculation of complexation energies of ethers with H_3O^+ has shown that the inclusion of only *polarization* nonadditivity exaggerates the interaction energy and unbalances it, such that the relative order of interaction energies of III and IV is reversed from those found experimentally. The additional inclusion of *exchange repulsion* nonadditivity, which has precedent in the work of Lybrand et al.[6] on alkali cation/$(H_2O)_2$ interactions, leads to much more reasonable absolute interaction energies and relative interaction energies qualitatively consistent with experiment.

The inclusion of such additional nonadditivity effects has also been further validated by comparison of quantum mechanical and molecular mechanical calculations on dimethoxyethane/H_3O^+ and dimethyl ether/H_3O^+ interactions. These model calculations show that the molecular mechanical calculations in which the exchange repulsion nonadditivity is not included might be expected to significantly overestimate the attractive interactions in H_3O^+ interactions with polyethers.

As a control on the addition of the three-body exchange term to the molecular mechanical force field, we also included calculations of the interaction of $(CH_3)_3NH^+$ with polyethers. In these cases, the three-body exchange term had little effect on the calculated interaction energies. Models that included polarization alone or polarization plus exchange repulsion nonadditivity lead to interaction energies in impressive agreement with experiment and are definite improvements over only two-body additive models.

An uncertainty in the comparison of the calculated energies with experiment is the uncertainty of which fragment is protonated and which is neutral. For example, it is known that I has a higher proton affinity than H_2O by about 20 kcal/mol;[34,35] thus, the

(34) Aue, D. H.; Bowers, M. T. In *Gas Phase Ion Chemistry*; Bowers, M. T., Ed.; Academic: New York, 1979; Vol. 2.
(35) (a) Sharma, R. B.; Blades, A. T.; Kebarle, P. *J. Am. Chem. Soc.* **1984**, *106*, 510. (b) Meot-Ner, M. *J. Am. Chem. Soc.* **1983**, *105*, 4906.

complex of the two molecules with a proton is certainly $I{\cdot}H^+/H_2O$ and not I/V. However, in the work described here, we have made the assumption that, in complexes involving the crown ethers II–IV with V–VII, V–VII remain protonated and II–IV are neutral. This is almost certainly a reasonable assumption for VII, where the proton affinity of the conjugate base is comparable to that of II–IV. The assumption is reasonable for VI, whose conjugate base proton affinity is comparable to II–IV, but it is less definite for V. The proton affinity of water is 173 kcal/mol,[34] whereas that of 18-crown-6 is 220–230 kcal/mol.[35] Thus, the observed ΔH of −88.5 kcal/mol[7a] for the IV/V interaction could be viewed as a ΔH of only approximately −33 kcal/mol for a $IV{-}H^+/H_2O$ interaction.

We thus created models of $IV{-}H^+$ based on the studies of Singh and Kollman[21] and then docked a TIP3P[36] water molecule to various sites on the crown ether and energy minimized the resulting structures. We never found interaction energies stronger than −13 kcal/mol for this complex. It also should be realized that the enhancement in the proton affinity of IV over I by ≈40 kcal/mol can be interpreted[21] as a stabilization of the $^{(+)}OH$ unit by the neighboring crown-O-dipoles, as seen in Figure 2 of ref 21. Thus, when a water molecule approaches, either such stabilizing interactions must be broken or the water must interact weakly and nonspecifically with the crown, leading to a weak interaction. On the other hand, H_3O^+ can interact strongly and effectively with a number of the oxygens of 18-crown-6 [Figure 1F].

(36) Jorgensen, W.; Chandresekhar, J.; Madura, J.; Impey, R.; Klein, M. J. *Chem. Phys.* **1983**, *79*, 926.

(37) **Note Added in Proof**: After this paper was accepted for publication, the first X-ray structure of IV/V was published [Atwood, J. L.; Bott, S. G.; Coleman, A. W.; Robinson, K. D.; Whetstone, S. B.; Means, C. M. *J. Am. Chem. Soc.* **1987**, *109*, 8110]. The structure clearly shows that the water molecule, not the ether, is protonated in the crystal. This supports the model for complexation used in this paper. The conformation found for IV in the crystal structure is similar to what we calculated (Figure 1); however, our calculations show a folding of one $-OCH_2CH_2O-$ fragment in the ether molecule resulting in enhanced interaction between IV and V over the more planar conformation of the crystal.

Our energies are not accurate enough to definitively prove the above analysis; extensive ab initio quantum mechanical optimization at the 6-31G* level would be required, which is beyond our current resources. The observation of the NH_4^+/18-crown-6[31] crystal structure is also supportive of our analysis, in that, in this condensed-phase case, it is clear that the proton resides on the hydride and not on the crown. Nonetheless, our assumptions of the protonation states have not been definitively proven, and this should be taken into account when judging our results.

The importance of including nonadditivity has been stressed before,[4,5] but recent precise gas-phase data have allowed one now to calibrate and precisely validate such models. It is clear from our studies of ethers alone, as well as their cation complexes, that nonadditive energy terms only become critical for ionic systems and are more important the smaller and more localized the ions.

Our procedure in adding polarization nonadditivity to standard molecular mechanical models is general, and one is now in a position to implement such models on complex biomolecules. At this point, we have only added the polarization energies after refinements with standard additive models, and we must now turn to algorithms in which the nonadditive energy is included during geometry optimization. Considerable technical work is still required to make such a process efficient enough so the computational overhead one must pay is not too severe. Nonetheless, with ever-increasing computer power, we see nonadditive empirical energy functions becoming of "routine" use in many simulations on ionic and biomolecular systems.

Acknowledgment. This work has been supported by the NSF [Grant CHE-85-10066] and NIH [Grant GM-29072]. The use of the UCSF Computer Graphics Laboratory [RR-1081] is also gratefully acknowledged.

Registry No. I, 115-10-6; I/V, 114273-93-7; I/VI, 114273-97-1; I/VII, 114274-01-0; II, 294-93-9; II/V, 114273-94-8; II/VI, 114273-98-2; II/VII, 114274-02-1; III, 33100-27-5; III/V, 114273-95-9; III/VI, 61040-12-8; III/VII, 114274-03-2; IV, 17455-13-9; IV/V, 98910-88-4; IV/VI, 32689-95-5; IV/VII, 114274-04-3; $(H_3COCH_2)_2/H_3O^+$, 114274-05-4; $(H_3COCH_2)_2$, 110-71-4.